KINETIC STUDY OF LIQUID-PHASE ADSORPTIVE REMOVAL OF HEAVY METAL IONS BY ALMOND TREE (*TERMINALIA CATAPPA* L.) LEAVES WASTE

[*]Michael Horsfall Jnr and Jöse L. Vicente

Instituto de Investigacions Fisicoquimicas Teorericas y aplicadas (INIFTA), Faculdad de Ciencias Exactas, Nacional Universidad de La Plata, 16 Surcural 1900, La Plata Argentina

ABSTRACT. The kinetic sorption of five metal ions - Al^{3+}, Cr^{6+}, Zn^{2+}, Ag^+ and Mn^{2+} - from aqueous solution onto almond tree leaves (ATL) waste in single component system has been studied. The experimental data was analyzed in terms of intraparticle diffusion and rate of adsorption, thus comparing transport mechanism and chemical sorption processes. The sorption rates based on the pseudo-second order rate constants for the five metal ions are 0.018 (Al^{3+}), 0.016 (Cr^{6+}), 0.023 (Zn^{2+}), 0.021 (Ag^+) and 0.022 (Mn^{2+}) g/mg.min. The adsorption rates are rapid and within 180 min of agitation more than 85 percent of these metal ions has been removed from solution by the ATL waste biomass. The kinetic data suggest that the overall adsorption process is endothermic, and that the rate-limiting step is a surface diffusion controlled process. The results from this study have revealed that the ATL waste, which is hitherto an environmental nuisance, has the ability to adsorb metal ions from solution and the data are relevant for optimal design of wastewater treatment plants. The low cost and easy availability of ATL waste make potential industrial application a strong possibility.

KEY WORDS: Kinetic sorption, Heavy metal ions, Almond tree leaves waste, Wastewater treatment plants

INTRODUCTION

Adsorption kinetic studies are important in predicting the rate of pollutant removal from aqueous systems. Kinetic studies provide information for selecting optimum operating conditions, identifying reaction pathways, understanding rate-limiting steps and are also essential for scaling-up of laboratory studies to industrial applications. The use of cheap adsorbents for the treatment of aqueous effluents to remove inorganic and organic pollutants has been recognized as a major development in the area of biosorption during the past ten years [1-10].

Some of the adsorbent studied for metal ions adsorption in aqueous solution includes modified groundnut husks (*Arachis hypogea)* [11], oil-palm fibres [12], sphagnum moss peat [13], tree fern [14], and waste tea leaves [15], just to mention a few. The literature search reveals that no information is presently available on kinetic study of metal ion removal by almond tree leaves waste.

The almond tree (*Terminalia catappa* L) has been known for its usefulness in the medical world. However, in Nigeria the almond tree is predominantly found and is known locally as "umbrella" tree because it gives shade for relaxation during hot weather. There are two extreme seasons in Nigeria, the dry and rainy seasons. During the rainy season the almond tree leaves are evergreen but begins to drop continuously during the dry season and therefore constitute environmental nuisance. In order to keep places like industries, schools and residential houses tidy of almond tree leaves waste, the wastes are gathered by cleaners/gardeners and are burnt regularly. This process releases dangerous gases into the atmosphere. In order to find solution to the waste liter, land pollution, as well as air pollution, the almond tree leaves waste was used for metal ion adsorption studies.

_____

*Corresponding author. E-mail: horsfalljnr@yahoo.com

This paper describes the adsorption kinetics of five metal ions (Al^{3+}, Cr^{6+}, Zn^{2+}, Ag^+, Mn^{2+}) in aqueous solution using almond tree leaves (ATL) waste. The kinetic models employed to fit the experimental data are discussed in terms of intra-particle diffusion and rate of adsorption.

EXPERIMENTAL

Sample collection and preparation

The adsorbent for this work is the almond tree (*Terminalia catappa* L) leaves (ATL) waste. The dried leaves were gathered into clean plastic bags. In order to ensure that homogeneous samples were collected, standard technique were applied. The air dried ATL wastes were further oven dried (Gallen Kamp, model OV-160, England) at 105 °C to constant weight and ground using a food processor (Magimax Cuisine System 5000) and then screened to obtain finely divided homogeneous particle size. The finely divided adsorbent was further soaked in 0.1 M HNO_3 acid for 48 h in order to remove all biogenic metals. This was followed by thoroughly washing with distilled water. The washing process continued until the filtrate gave a negative EDTA test for heavy metal ions. The test was carried out by the addition of 5 drops of 0.01 M EDTA solution and 2 mL of NH_3/NH_4Cl buffer to 5 mL of the washing water filtrate. The appearance of blue colour of the EDTA solution indicates that the biomass does not contain metal ions. The filtered biomass was then oven-dried to constant weight at 45 °C and finally grounded and sieved again. The fraction with size < 100-μm was collected for use in the batch-adsorption studies, which was stored in clean, air tight plastic containers until ready for use.

Adsorbent characterization

The physico-chemical characteristic of the adsorbent was determined using standard procedures. Proximate analysis was carried out using standard method [13]. The finely divided adsorbent was characterized for apparent density, porosity, pore volume, ash content, volatile matter, surface area, moisture content and Sodium capacity. The specific surface area was measured by the Brunauer-Emmett-Teller (BET) N_2 adsorption isotherm technique using a Quantasorb surface analyzer (Model-05) at 77.15 K. The sodium capacity was determined by contacting 200 mg of the ATL adsorbent with 25 mL of 0.1 M NaOH and the resultant mixture was allowed to equilibrate on a shaker for 72 h. The resultant mixture was filtered to remove the adsorbent and 20 mL of the filtrate was pipette out and back titrated using 0.1 M HCl and phenolphthalein as an indicator. The Na^+ content was computed accordingly.

Batch experimental procedure

The adsorbate stock solutions of 1000 mg/L metal ions of Al^{3+} (from $Al(NO_3)_3$), Cr^{6+} (from $K_2Cr_2O_7$), Zn^{2+} (from $ZnCl_2$), Ag^+ (from $AgNO_3$) and Mn^{2+} (from $MnSO_4$) were prepared by dissolving appropriate amount of each salt in 1000 mL of double distilled deionized water. Batch mode adsorption studies were carried out with 1.0 g of adsorbent and 100 mL of 80 mg/L metal ion solution at a fixed pH of 5.0 in 250 mL conical flasks and kept at a temperature of 30 °C in a water bath with a stirrer set at 200 rpm. The mixtures were equilibrated at time intervals of 10, 20, 30, 40, 50, 60, 70, 80, 90, 100, 110, 120, 130, 140, 150, 160, 170, 180, 200, 220, 240, 260, 280, 300 min. At the end of each time interval, the suspension was allowed to settle followed by centrifugation at 2500 rpm for 5 min and then decanted. Aliquots (1 mL) of the supernatant solutions were withdrawn and acidified with 1 % nitric acid solution for residual metal ions estimation. The final solution concentration C_o was determined by FAAS (model 200

A), leading to the calculation of the metal sorption uptake (q_e) for each metal-ATL adsorption system using the general formula of Volesky [16]:

$$q_e = \frac{v}{m}(C_o - C_e) \tag{1}$$

where q_e is metal ion concentration on the adsorbate (mg/g) at equilibrium, C_o and C_e are the initial and equilibrium metal ion concentrations (mg/L) in solution of volume v (mL) and m is the mass of adsorbate used (g).

The calibration was performed within the range for each metal. Controls of one of the metal solution were run to detect any possible metal precipitation or contamination. The confidence level of the result was 95 %. Triplicate determinations were made for each determination and their mean values computed for quality assurance.

RESULTS AND DISCUSSION

Physical and surface characteristics

The data in Table 1 gives some physical characteristics of the almond tree leaves (ATL) waste biomass. These characteristics play some important role in the adsorption process of metal ions onto the biomass. The low value of the apparent density (1.2 ± 0.06 g/cm³) is an indication of the ease of suspension of the biomass in aqueous solution, which is an essential factor in the interaction between metal ion in solution and the ligand on the biomaterial. Apparent density closer to unity indicates higher contact between adsorbate and adsorbent. The porosity and pore volume are important factor in characterizing the microstructure properties of the biomass. The porosity and pore volume of the almond tree leaves biomass are 43.3 ± 0.08 % and 0.8 ± 0.02 cm³/g. The moisture and ash contents are relatively low, which further indicates the high suspendability in aqueous phase, while a high level of volatile matter supports these reasoning. The specific surface area was found to be 68.4 ± 0.31 m²/g. Sodium capacity determination shows that the affinity of the Na^+ ions for the biomass is 0.4 ± 0.04 mmole/g. Sodium uptake is determined in order to evaluate the total sorption capacity of the biomass for cations. According to Chingombe and co-workers [17], the sodium uptake is caused by the presence of weakly acidic functional groups on the adsorbent surface, which in liquid phase may easily dissociate and serve as sorption or ion exchange sites for metal ions.

Table 1. Some physical characteristics of the ATL waste biomass[*].

Parameters	Values
Apparent density, g/cm³	1.2 ± 0.06
Porosity, %	43.3 ± 0.08
Pore volume, cm³/g	0.8 ± 0.02
Ash content, %	12.3 ± 0.11
Volatile matter, %	84.2 ± 1.06
Surface area, m²/g	68.4 ± 0.31
Moisture content, %	9.1 ± 0.47
Sodium capacity, mmole/g	0.4 ± 0.04

[*]Values are given as mean of triplicate measurements and standard deviations.

Effect of contact time

Available adsorption results revealed that the uptake of adsorbate species is fast at the initial stages of the contact period, and thereafter, it becomes slower near the equilibrium. In between these two stages of the uptake, the rate of adsorption is found to be nearly constant. This is obvious from the fact that a large number of vacant surface sites are available for adsorption during the initial stage, and after a lapse of time, the remaining vacant surface sites are difficult to be occupied due to repulsive forces between the solute molecules on the solid and bulk phase. In order to study the effect of time, aqueous solutions of the five metal ions (Al^{3+}, Cr^{6+}, Zn^{2+}, Ag^+, Mn^{2+}) containing a fixed concentration of 80 mg/L were kept in contact with the almond tree leaves (ATL) waste adsorbent for different time intervals from 10-300 min and the data are presented in Figure 1.
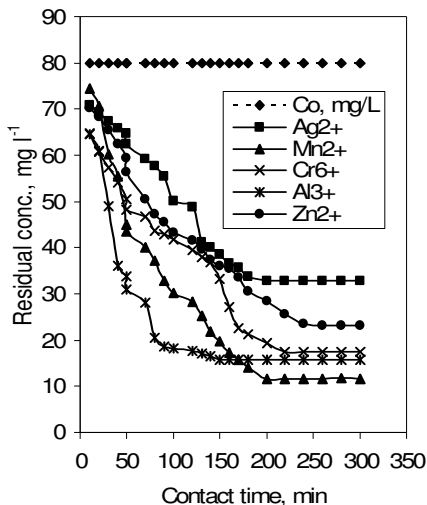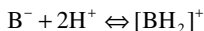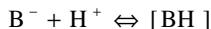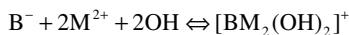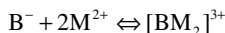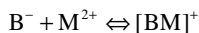

Figure 1. Adsorption isotherms for the four metal ions on ATL. C_o is initial concentration of metal ions.

The data showed a rapid drop in the amount of initial metal ion concentration remaining after each time interval until about 110 min. No significant change in the removal of Al^{3+} is observed after 80-90 min, while the observed removal trends for the other four metals (Cr^{6+}, Zn^{2+}, Ag^+, Mn^{2+}) is about 120-160 min. It was found that adsorptive removal of each metal reached equilibrium at 180 min of contacting with the ATL adsorbent. The time of 180 min indicates the residence time required for maximum removal of these metal ions by ATL adsorbent. According to Gardea-Torresdey and co-workers [18], a long contact time necessary to reach equilibrium indicates that the predominant mechanism is physical adsorption, while short contact time indicates chemisorption. The relatively long contact times observed for the ATL-metal ion systems observed in this investigation indicates that physisorption is probably the predominant mechanism. Since the solubility of a metal ion is an important factor, which enables metal ions to penetrate into the porous structure of the biomaterial, the solution equilibria for the biomaterial and a divalent metal ion could be represented as shown below:

$$B^- + H^+ \Leftrightarrow [BH]$$

$$B^- + 2H^+ \Leftrightarrow [BH_2]^+$$

$$B^- + M^{2+} \Leftrightarrow [BM]^+$$

$$B^- + 2M^{2+} \Leftrightarrow [BM_2]^{3+}$$

$$B^- + M^{2+} + OH^- \Leftrightarrow [BMOH]$$

$$B^- + 2M^{2+} + 2OH \Leftrightarrow [BM_2(OH)_2]^+$$

Kinetic treatment of the sorption process

The kinetic treatment of the experimental data is discussed in terms of intra-particle diffusion and rate of adsorption.

Intra-particle diffusion study

The transport of adsorbate from the liquid phase to the adsorbent surface occurs in several steps. This may include film or external diffusion, pore diffusion, and surface diffusion. The intra-particle diffusion of the metal ion-ATL adsorption process was assessed using three models which include fractional attainment of equilibrium (FAE), linear driving force (LDF) and Weber-Morris diffusion model. Intra-particle diffusion rate orders are simple-first-order reaction models of the type

$$A \underset{k_b}{\overset{k_f}{\Leftrightarrow}} B \tag{2}$$
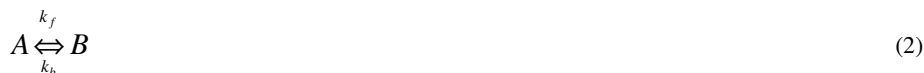
where K_f is the forward reaction rate constant and K_b is the backward reaction rate constant. If a is the initial concentration of adsorbate and x is the amount transferred from liquid phase to solid phase at any time t, then the rate can be expressed as

$$\frac{dx}{dt} = -\frac{d(a-x)}{dt} = k(a-x) \tag{3}$$

where k is the overall rate constant. Since K_f and K_b are the rate constants for the forward and reverse process, the rate can be expressed as

$$\frac{dx}{dt} k_f(a-x) - k_b x \tag{4}$$

If X_e represents the concentration of adsorbate at equilibrium, then at equilibrium we have that $K_f(a-x_e) - K_b X_e = 0$, and under these conditions:

$$\frac{dx}{dt} = 0 \quad \text{or} \quad k_c = \frac{X_e}{a - X_e} = \frac{k_f}{k_b} \tag{5}$$

where K_c is the equilibrium constant. Hence, at equilibrium conditions, the rate becomes

$$\frac{dx}{dt} = [k_f(a-x) - k_b x] - [k_f(a - X_e) - k_b X_e] \tag{6}$$

The above equation is in the form $\dfrac{dx}{dt} = k(a-x)$. Therefore

$$k_f + k_b = \frac{1}{t}\ln\frac{X_e}{X_e - x} \tag{7}$$

Then

$$\ln(1 - U) = -(k_f + k_b)t = -kt = -k_f\left[1 + \frac{1}{k_c}\right] \tag{8}$$

where $U = \dfrac{x}{X_e}$ and k is the overall rate constant.

Equation 8 is the intra-particle diffusion equation which has been applied in different ways by different authors.

The kinetic theory behind the fractional attainment of equilibrium (FAE) is that it can be used to explain the adsorption process in terms of adsorption being controlled by film-diffusion. The fractional attainment of equilibrium equation [19] is expressed as

$$\ln(1 - \alpha) = -kt \tag{9}$$

where α is the fractional attainment of equilibrium. It is the ratio of the amounts of metal ion removed from solution after a certain time (C_t) to that removed when sorption attained equilibrium (C_e), and k is the overall rate constant. In order to quantify the fractional attainment of equilibrium to the experimental data, a plot of $\ln(1-\alpha)$ against time (t) was made (Figure 2). According to Vinod and Anirudhan [19], a non-linear relationship between the plot of $\ln(1-\alpha)$ versus (t) indicates that the diffusion of adsorbate onto the adsorbent surface is film-diffusion controlled. In such condition, an external factor such as high agitation speed may be required to break the diffusion barrier and increase adsorbate-adsorbent interaction. The plot in Figure 2 is non-linear and showed more than one step. The data shows that film diffusion controlled process may possibly be a factor in the ability of metal ions to migrate to ATL surface.
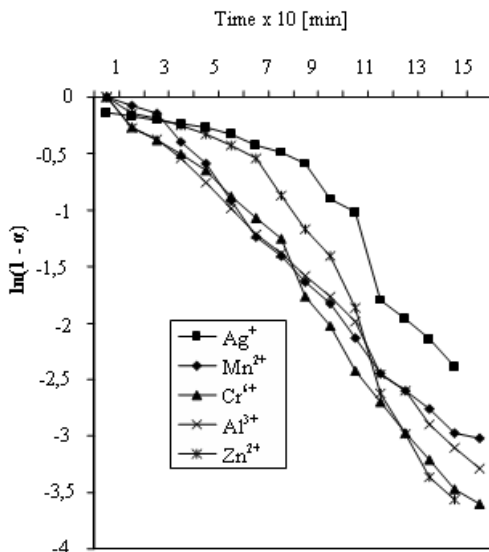

Figure 2. The FAE plot for the metal ions-ATL system.

The theoretical basis behind the linear driving force (LDF) is the ability to quantitatively explain the restrictions of adsorbate into the pores of the adsorbent. The LDF mass transfer kinetic model equation is described as follows

$$\frac{q_t}{q_e} = 1 - \exp(-kt) \tag{10}$$

where q_t and q_e are the amounts of metal adsorbent at time (t) and at equilibrium and k is the overall rate constant. The rate constant can be determined from the gradient of the graphs of $\ln(1 - q_t/q_e)$ versus t, after linearizing Equation 10 to Equation 11 $\ln(1 - q_t/q_e)$

$$\ln(1 - \frac{q_t}{q_e}) = -kt \tag{11}$$

Whether the adsorption kinetics follows a LDF or not depends on the diameter of the adsorbate relative to the porosity of the material. When the rate-limiting step is pore diffusion, then there is a barrier at the pore entrance. Thus, the degree of fitting of the data to the LDF model gives an indication of the evolution of the porous texture of the samples. The LDF plot for the metal ions-ATL system is shown in Figure 3. The data shows that pore diffusion controlled rate-limiting mechanism into the porous structure of the ATL is not applicable for the five metal ions investigated. However, careful examination of the plots in Figure 3 showed that Zn^{2+}, Al^{3+} and Cr^{6+} are more linear than the other metals probably due to their smaller ionic radii.
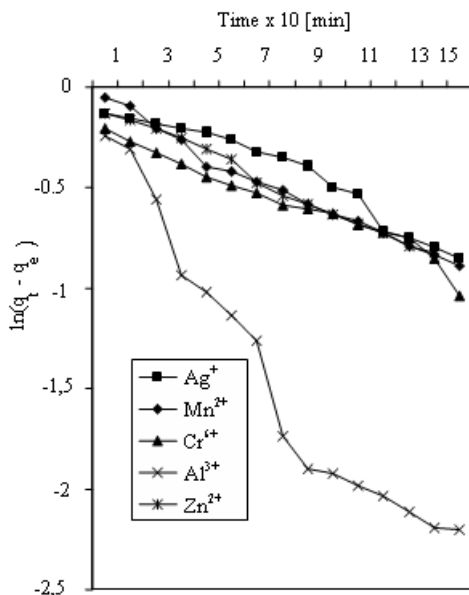

Figure 3. The LDF plot for the metal ions-ATL system.

The possibility of intra-particle diffusion was also explored by the Weber-Morris model equation [20]

$$q_t = kt^{0.5} + C \tag{12}$$

where k is the rate constant (mg g^{-1}min$^{-0.5}$) and C is a constant that gives idea about the thickness of the boundary layer. According to Weber and Digiano [20], if the Weber-Morris plot of q_t vs $t^{0.5}$ gives a straight line, then the adsorption process is controlled by surface diffusion only. However, if the data exhibit multi-linear plots, then two or more steps influence the adsorption process. The mathematical dependence of the uptake of the adsorbate on $t^{0.5}$ is presented in Figure 4. The plot shows a curvature for the initial period, usually attributed to boundary layer diffusion effects or external mass transfer effects [21, 22]. The multi-linearity of the plots indicates the presence of two or more steps taking place. The first, sharper portion is the instantaneous adsorption stage or external surface adsorption, the second portion is the gradual adsorption stage where intra-particle diffusion is rate-limiting and the third portion is the final equilibrium stage where intra-particle diffusion starts to slow down due to extremely low metal ion concentration left in the solution. Closer examinations of these plots show that the third stage is the predominantly rate-limiting step. Extrapolation of the linear portions of the *y*-axis gives the intercepts, which provide the measure of the boundary layer thickness. The deviation of the straight lines from the origin (Figure 4) may be due to difference in rate of mass transfer in the initial and final stages of adsorption. Furthermore, such deviation of straight line from the origin indicates that the pore diffusion is not the rate-controlling step. The larger the value of C the greater is the boundary layer effect [23]. The values of rate constants (k) and the boundary effects are shown in Table 1. The data shows that the boundary effect for Ag$^+$ is larger than the other metals probably due to its relatively larger ionic radius when compared to the other metals investigated.
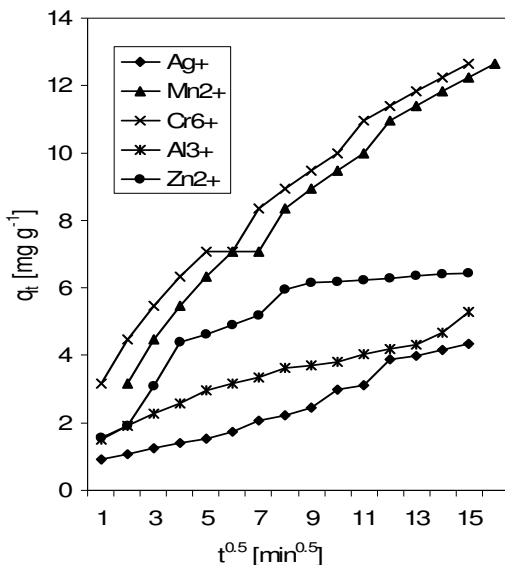

Figure 4. Plot of Weber-Morris model for the metal ion-ATL system.

Table 1. Intra-particle diffusion rate constants k, coefficient of determination r^2 and the boundary layer effect constants C for the three models

Models		Metals				
		Al^{3+}	Cr^{6+}	Zn^{2+}	Ag^+	Mn^{2+}
FAE	k, min^{-1}	0.222	0.257	0.267	0.165	0.225
	r^2	0.993	0.983	0.906	0.851	0.991
LDF	k, min^{-1}	0.150	0.029	0.057	0.054	0.059
	r^2	0.935	0.963	0.992	0.946	0.986
W – M	k, min^{-1}	0.230	0.656	0.330	0.265	0.656
	r^2	0.972	0.983	0.814	0.973	0.983
	C	0.814	1.585	2.724	3.380	0.374

FAE = fractional attainment of equilibrium, LDF = linear driving force, W-M = Weber/Morris.

Determination of adsorption rate constants

The adsorption of metal ion from a liquid phase onto a solid phase is a reversible process. The pseudo-first order kinetic can be expressed by the differential equation as follows [9]

$$\frac{dq_t}{dt} = k_1(q_e - q_t) \qquad (13)$$

Integrating the above equation for the boundary conditions $t = 0$ and $q_t = q_e$ gives

$$\log(q_e - q_t) = \log q_e - \frac{k_1}{2.303}t \qquad (14)$$

which is the integrated rate law for a pseudo-first order reaction, where q_e is the amount of metal ion adsorbed at equilibrium (mg/g), q_t is the amount of metal ion adsorbed at time t (mg/g) and k_1 is the equilibrium rate constant of pseudo-first order adsorption (min^{-1}). In order to obtain the rate constants, straight line plots of log (q_e - q_t) against t for different metals at 30 ^{o}C were made (Figure 5). The rate constants, k_1 and the coefficient of determinations (r^2) values (Table 2) of the metals were computed from the plots. Non-linear fits were observed for all the metals, indicating that adsorption reaction between these metals and ATL may not be appropriately approximated by the pseudo-first order kinetics.

Table 2. Rate law constants and activation energy for the five metal ions on ATL waste.

| Models		Metals				
	Units	Al^{3+}	Cr^{6+}	Zn^{2+}	Ag^+	Mn^{2+}
Pseudo-1st	k_1 (min^{-1})	0.013	0.004	0.005	0.005	0.005
	q_e, (mg/g)	5.18	6.71	7.23	7.50	9.95
	r^2	0.912	0.950	0.984	0.963	0.967
Pseudo-2nd	k, ($g/mg.min$)	0.018	0.016	0.023	0.021	0.022
	h_o($mg/g.min$)	1.46	1.23	2.01	1.06	1.50
	q_e, (mg/g)	9.01	8.27	9.35	7.09	8.26
	r^2	0.992	0.982	0.992	0.982	0.990
Elovic	k_1 (min^{-1})	1.99	0.78	1.33	1.34	2.26
	a (mg/g)	4.59	2.88	3.30	3.07	5.07
	r^2	0.945	0.935	0.927	0.891	0.972
ΔE_a	$kJ/molK$	11.08	10.94	10.26	9.88	10.64
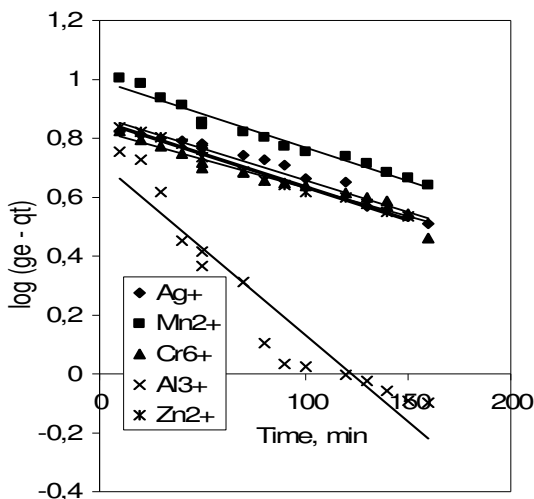
Figure 5. Linear plot representing pseudo-first order rate model for metal ion-ATL complex

A pseudo-second order model [2, 8] was also used to describe the kinetics of adsorption of metal ions on ATL waste. Here it is assumed that the adsorption capacity is proportional to the number of binding sites occupied on the adsorbent, and then the kinetic rate law can be rewritten as follows

$$\frac{dq_t}{dt} = k_2(q_e - q_t)^2 \tag{15}$$

where k_2 is the rate constant of adsorption (g/mg.min), q_e is the amount of metal ion adsorbed at equilibrium (mg/g), q_t is the amount of metal ion adsorbed at time t (mg/g). Integrating Equation 15 for the boundary conditions $t = 0$, $t = t$ and $q_t = 0$ to $q_t = q_t$ gives

$$\frac{t}{q_t} = \frac{1}{k_2 q_e^2} + \frac{1}{q_e} t \tag{16}$$

Which is the integrated rate law for a pseudo-second order equation. The initial adsorption rate, as t $\rightarrow$ 0 can be defined by the Ho-constant (h_o) [2] as follows

$$h_o = k_2 q_e^2 \tag{17}$$

The initial adsorption rate, h_o, the equilibrium adsorbed amount, q_e, the pseudo-second order rate constant, k_2, and the coefficient of determinations (r^2) were determined experimentally from the slope and intercept by plotting t/q_t versus t as shown in Figure 6. The data as plotted in Figure 6 show better fits for all the metals, indicating that the adsorption reaction can be more appropriately described with the pseudo-second order kinetic model. The constants were calculated from the plots and are presented in Table 2. It can be observed that h_o (the initial sorption rate, (g/mg.min), is higher for Al^{3+} and Cr^{6+} than the other metals. This is an indication that initial adsorption of these two metals by ATL biomass was faster and in a mixture of metals of this group, Al^{3+} and Cr^{6+} may be quantitatively removed before others.
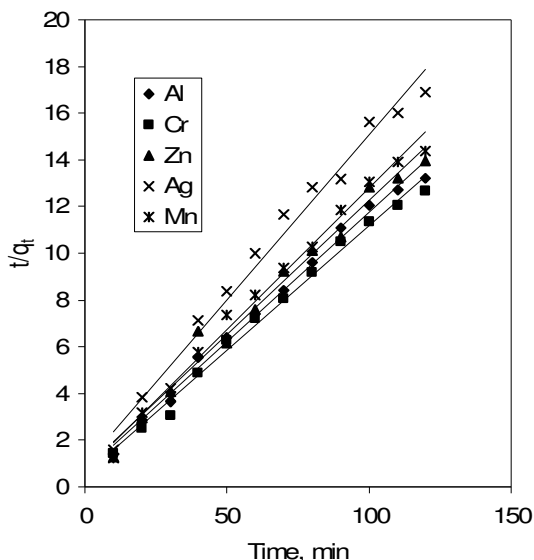
Figure 6. Linear plot of pseudo-second order rate for metal ion-ATL complex.

In liquid phase adsorption reactions, the rate decreases with time due to an increase in surface coverage. One of the most useful models for describing such condition is the Elovic model [24]

$$\frac{dq_t}{dt} = a \exp(kq_t) \tag{18}$$

where a and k are constants during any one experiment. The constant a is regarded as the initial rate because $dq_t/d_t \rightarrow a$ as $q_t = 0$. Given that $q_t = 0$ at $t = 0$, the integrated form of Equation 18 becomes

$$q_t = \frac{1}{k}\ln(t + t_o) - \frac{1}{k}\ln t_o \tag{19}$$

where $t_o = 1/ak$. If $t > t_o$, Equation 19 is simplified as

$$q_t = \frac{1}{k}\ln(ab) + \frac{1}{k}\ln t \tag{20}$$

The applicability of the Elovic model equation to the experimental data was tested by constructing linear plot (Figure 7) of q_t versus log t after simplifying natural logarithm of Equation 20 to $\log_{10}$ as follows:

$$\log q_t = a + 2.303\,k\log t \tag{21}$$

Based on the r^2 values obtained (Table 2). It was observed that Elovic equation failed to give good fittings to the experimental data for the adsorption of Al^{3+}, Cr^{6+}, Zn^{2+}, Ag^+, Mn^{2+} on ATL.
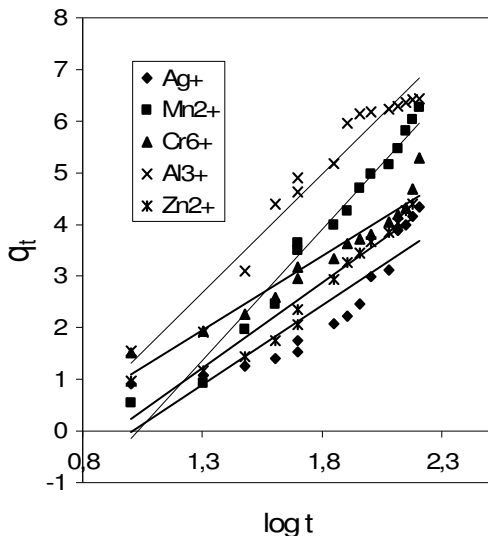
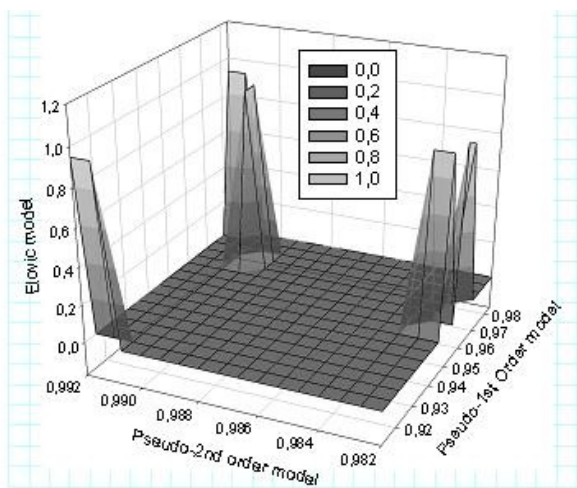Figure 7. Linear plot of the Elovic rate model for the metal ions on ATL.

Figure 8. A 3D bar chart of the r^2 values from the three rate constant models.

Goodness of fit of kinetic models

It has been suggested that linearization plots may not be a significant basis to reject or accept a model. To further analyze the suitability of the three (pseudo-first order, pseudo-second order and Elovic equation) models, their fit to the experimental data was assessed. The fit of the data was established using a single statistical parameter (r^2) which is called the coefficient of determination. The coefficient of determination values for the three models as shown in Table 2

shows that the three models are applicable in describing the data (as all $r^2 > 0.90$) with pseudo-second order more appropriate. This observation is further depicted in a 3D bar chart plot (Figure 8). As a fit becomes more ideal, the r^2 values approach 1.0 with 0 representing a complete lack of fit. The significance of the independent variable r^2 in each model was further tested using the F-test as defined by ANOVA. The F-statistic was used to test the null hypothesis that the variances of the three models are equal. The mean square error or the variance of the random errors (Table 3) indicates that the pseudo-second order kinetic model fits the experimental data more that the other models. However, the F-statistic shows no significant difference (at $p < 0.05$) in the ability of the three models in describing the experimental data.

Table 3. Two-way analysis of variance without replication.

A. Summary	Count	Sum	Average	Variance
Ag^{2+}	3	2.836	0.945333	0.002304
Mn^{2+}	3	2.929	0.976333	0.000146
Cr^{6+}	3	2.867	0.955667	0.000576
Al^{3+}	3	2.853	0.951	0.001603
Zn^{2+}	3	2.903	0.967667	0.001256
Pseudo-1	5	4.776	0.9552	0.000731
Pseudo-2	5	4.938	0.9876	2.68E-05
Elovic	5	4.674	0.9348	0.000891

b. ANOVA						
Source of Variation	SS	df	MS	F	P-value	F crit
Metals	0.001912	4	0.000478	0.816445	0.549131	3.837854
Models	0.00709	2	0.003545	6.055519	0.025039	4.458968
Error	0.004683	8	0.000585			
Total	0.013684	14				

Evaluation of activation energy

The adsorption rate constant was used to evaluate the activation energy, using an Arrhenius form equation expressed by the following relationship [25]:

$$k_2 = k_o \exp(-\frac{E_a}{RT}) \qquad (22)$$

where k_2 is the pseudo-second order adsorption equilibrium constant, g/mg min, k_0 is initial rate constant for pseudo-second order, E_a is activation energy, R is the gas constant (8.314 J/k mol) and T is absolute temperature (K). k_0 may be related to h_o, hence equation 22 may be rewritten as:

$$k_2 = h_o \exp(-\frac{E_a}{RT}) \qquad (23)$$

The linear form of the Arrhenius-like expression was applied to our experimental data (equation 24):

$$\ln k_2 = \ln h_o - \frac{E_a}{RT} \qquad (24)$$

The values of E_a were computed from equation 24 at *ca.* 30 °C and are presented in Table 2. The activation energies are positive indicating an endothermic reaction, meaning that small amount of energy is required by the sorption system and that temperature increase may enhance the sorption process.

CONCLUSIONS

We have in a batch experimental procedure studied the kinetic liquid-phase adsorptive removal of Al^{3+}, Cr^{6+}, Zn^{2+}, Ag^+, and Mn^{2+} ions by almond tree (*Terminalia catappa* L.) leaves waste. The kinetics of the adsorption process was found to reveal that the overall transport mechanism of adsorbate to the adsorbent surface is a combination of film, pore and surface diffusions with adsorption on the adsorbent surface as the predominantly the rate-limiting step of the process and follows a pseudo-second order rate law. The adsorption rate constants for the metal ions investigated in each mode is consistent. The reaction process was found to be endothermic. This investigation has shown that almond tree leaves waste which is hitherto an environmental nuisance could be converted to cheap and environment friendly adsorbent for pollutant remediation in effluents.

AKNOWLEDGEMENTS

REFERENCES

1. El-Geundi, M.S. *Wat. Res.* **1991**, 24, 271.
2. Ho, Y.S.; Wase, D.A.J.; Forster, C.F. *Wat. Res.* **1995**, 29, 1327.
3. Ho, Y.S.; McKay, G.; Wase, D.A.J.; Forster, C.F. *Adsorpt. Sci. Technol.* **2000**, 18, 639.
4. Horsfall Jr., M.; Spiff, A.I.; Abia, A.A. *Bull. Korean Chem. Soc*. **2004**, 25, 969.
5. Horsfall Jr., M.; Abia, A.A. *Wat. Res.* **2003**, 37, 4913.
6. Horsfall Jr., M.; Spiff, A.I *Chem. Biodiv*. **2005**. 2, 373.
7. Horsfall Jr., M.; Ogban, F.; Akporhonor, E.E. *Chem. Biodiv*. **2005**, 2, 1246.
8. Horsfall Jr., M., Spiff, A.I. *Bull. Chem. Soc. Ethiop*. **2005**, 19, 89.
9. Quek, S.Y.; Wase, D.A.J.; Forster, C.F. *Water SA* **1998**, 24, 251.
10. Sun, G.; Weixing S. *Ind. Eng. Chem. Res*. **1998**, 37, 1324.
11. Okiemen, F.E.; Okundia, E.U.; Ogbeifun, D.E. *J. Chem. Technol. Biotechnol.* **1991**, 51, 97.
12. Low, K.S.; Lee, C.K.; Lee, K.P. *Biores. Technol.* **1993**, 44, 109.
13. Ho, Y.S.; McKay, G. *Wat. Res.* **2000**, 34, 735.
14. Ho, Y.S.; Chiu, W.T.; Hsu, C.S.; Huang, C.T. *Hydrometallurgy* **2004**, 73, 55.
15. Tan, W.T.; Khan, R.M. *Environ. Technol. Let.* **1988**, 9, 1223.
16. Volesky, B. *Biosorption and biosorbents* in *Biosorption of Heavy Metals*, Volesky, B. (Ed.), CRC Press: Boca Raton; **1990**; pp 3-5.
17. Chingombe, P.; Saha, B.; Wakeman, R. *J. Carbon* **2005**, 43, 32.
18. Gardea-Torresdey, J.L.; Tang, L.; Salvador, J.M. *J. Hazard. Mater.* **1996**, 48, 191.
19. Vinod, V.P.; Anirudhan, T.S. *J. Chem. Technol. Biotechnol.* **2002**, 77, 92.
20. Weber Jr., W.J.; Digiano, F.O. *Process Dynamics in Environmental System*; Environmental Science and Technology Series, John Wiley and Sons: New York; **1996**; pp 89-94.
21. McKay, G.; Otterburn, M.S.; Sweeney, A.G. *Wat. Res.* **1980**, 14, 15.
22. Srivastava, V.C.; Swamy, M.M.; Mall, I.D.; Prasad, B.; Mishra, I.M. *Colloids and Surfaces A: Physicochem. Eng. Aspects* **2006**, 272, 89.
23. Kannan, K.; Sundram, M.M. *Dyes Pigments* **2001**, 51, 25.
24. Goswami, S.; Ghosh, U.C. *Water SA* **2005**, 31, 597.
25. Ofomaja, A.E.; Ho, Y.S. *J. Hazard. Mater.* **2005**, 120, 157.